The relative acceptor and donor emission intensity is then given by

$$\frac{F_a}{F_d} = \frac{q_a}{q_d}\frac{(k_a + k_d E)}{k_d(1-E)}\frac{(1+R_\infty'')(e^{2b's'L} - R_\infty'^2)f_A}{(1+R_\infty')(e^{2b''s''L} - R_\infty''^2)f_D} \quad \text{(A7)}$$

where f_A and f_D are given by eqs 2b and 2a, respectively.

The acceptors excited by absorbing the donor fluorescence can reemit fluorescence to return to their ground states. In the absence of scattering and absorption of the reemitted fluorescence, the contribution to the observed acceptor fluorescence due to this radiative energy transfer in layer dx is

$$dP_A = \frac{dF_d}{2} q_a k_a' \int_0^x \frac{(1+R_\infty')[e^{b's'(2L-y)} - R_\infty' e^{b's'y}]}{[e^{2b's'L} - R_\infty'^2]}\,dy \quad \text{(A8)}$$

Using eqs 1 and A1 and integrating over the thickness L, we found

$$P_A = I_0 q_a k'_a (1-E)(1+R_\infty) \times (1+R_\infty')\frac{\alpha}{2b's'(e^{2bsL} - R_\infty^2)(e^{2b's'L} - R_\infty'^2)} \quad \text{(A9)}$$

where α is given by eq 2c. Equation A7 is thus modified to give eq 2.

References and Notes

(1) Morawetz, H. *Science* **1988**, *240*, 172. Stryer, L. *Annu. Rev. Biochem.* **1978**, *47*, 819. Steinberg, I. Z. *Annu. Rev. Biochem.* **1971**, *40*, 83.
(2) Forster, Th. *Ann. Phys. (Leipzig)* **1948**, *2*, 55.
(3) Stryer, L. *Science* **1968**, *162*, 526.
(4) Horsky, J.; Morawetz, H. *Macromolecules* **1989**, *22*, 1622.
(5) Melhuish, W. H. In *Optical Radiation Measurements*; Academic Press: New York, 1982; Vol. 3, Chapter 5.
(6) Amrani, J.; Huang, M.; Morawetz, H. *Macromolecules* **1980**, *13*, 649.
(7) Albert, B.; et al. *Macromolecules* **1985**, *18*, 388.
(8) Fredrickson, G. H. *Macromolecules* **1986**, *19*, 441.
(9) Kubelka, P. *J. Opt. Soc. Am.* **1948**, *38*, 448.
(10) Allen, E. *J. Opt. Soc. Am.* **1964**, *54*, 506.
(11) Jachowicz, J.; Morawetz, H. *Macromolecules* **1982**, *15*, 828.

Degradation of Polymer Solutions in Extensional Flows

Jeffrey A. Odell,* Alejandro J. Muller, Kwabena A. Narh, and Andrew Keller

H. H. Wills Physics Laboratory, University of Bristol, Tyndall Avenue, Bristol BS8 1TL, England

Received July 31, 1989; Revised Manuscript Received December 13, 1989

ABSTRACT: Elongational flow techniques are applied to the examination of flow-induced chain scission of macromolecules in solution. An opposed-jets apparatus is used both to produce mechanical scission and to monitor the molecular weight distribution of the scission products. We have explored the combined effects of elongational flow and elevated temperatures upon degradation of almost monodisperse atactic polystyrene solutions. Between 25 and 150 °C degradation occurs as closely central scission of the molecules beyond a critical strain rate ($\dot{\epsilon}_f$). $\dot{\epsilon}_f$ is found to be a decreasing function of temperature. At 150 °C we present also results for thermal degradation alone. These results correlate well with predictions based upon a thermally activated barrier to scission (TABS) model. We also present results on the strain-rate dependence of the scission rate beyond $\dot{\epsilon}_f$ at room temperature. These results clearly indicate that in dilute solution only those molecules that are virtually fully stretched can undergo central scission. Degradation in real flow situations (for instance, flow through GPC columns) seems to parallel our idealized experiments. Our results have serious implications for the latest theories of polymer dynamics. Finally, we speculate that, contrary to common belief, simple laminar shear flows may be almost incapable of degrading polymer solutions and that degradation is only encountered when the flow contains an appreciable elongational component, commonly arising as a result of flow instabilities or turbulence.

1. Introduction

Stress-induced scission of polymers in solution is a subject of major theoretical and technological interest. The thermochemical nature of mechanically induced scission of polymers has attracted the attention of many theorists since the pioneering works of Kuhn and Frenkel.[1,2] These authors over 40 years ago pointed out that long-chain molecules can be stretched out and broken if the stress applied exceeds the breaking stress of the fundamental chemical bonds. Technologically, the use of polymer solutions for flow modifications (in drag reduction or viscosity enhancement for example) is limited mostly by mechanically and/or thermally induced scission of the chains.

The breakage of chains in dilute solution can be studied by elongational flow.[3-8] Stagnation-point extensional flow fields can effectively apply a controlled stress to the isolated molecule. Simultaneously, the conformation of the molecule can be monitored by a variety of optical techniques. Using elongational flow techniques, one can vary both the stress and the temperature applied to the molecules in order to study their vital influence in the flow-induced scission process.

In an elongational flow field an isolated flexible-chain molecule is expected to undergo a coil-stretch transition at a critical strain rate, $\dot{\epsilon}_c$. This is a prediction from theoretical considerations,[9-11] being due to the hysteresis of molecular relaxation time with chain extension. The critical strain rate is related to the longest relaxation time of the molecule (τ) as

$$\dot{\epsilon}_c \tau \approx 1 \quad (1)$$

Extensional flow fields have been realized experimentally by a number of devices, cross slots, opposed jets,

0024-9297/90/2223-3092$02.50/0

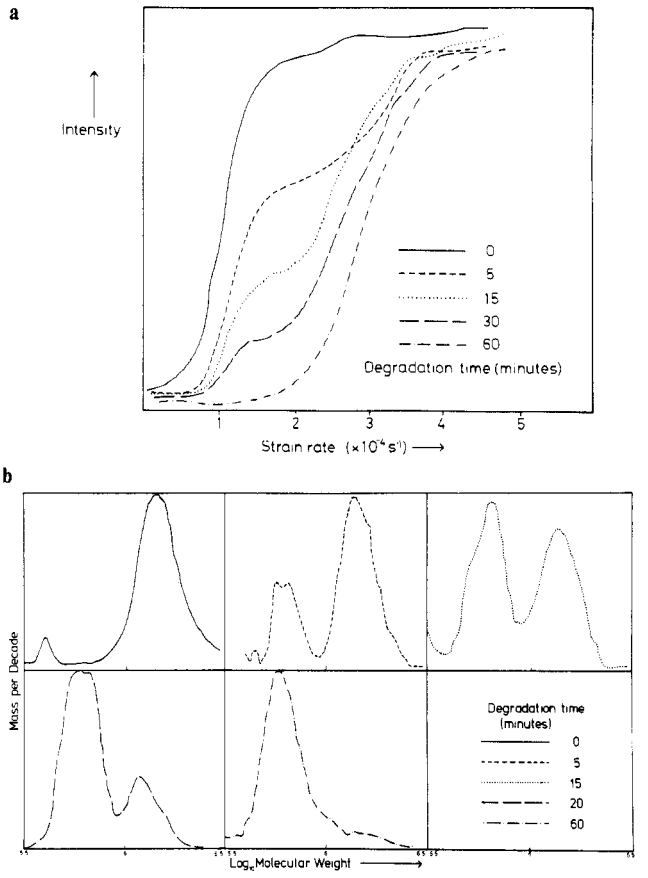

Figure 1. (a) Progressive change with time of the birefringent intensity vs strain rate curve of a PEO solution that is subject to overstretching at 5×10^5 s^{-1} in the cross-slot apparatus (initially, a 0.1% solution of 1.4×10^6 M_w PEO in water). (b) The molecular weight distribution curves derived from (a) as the polymer molecules are progressively degraded.

and four-roll mills.[4] Such devices produce almost pure extensional flow fields and incorporate a stagnation point at their center of symmetry. The extension of molecules can be assessed from optical retardation in the solution. As strain rate is increased a narrow birefringent line is observed around the stagnation point. This localization of extension is a consequence of the large strain required to highly extend high molecular weight flexible molecules: such large strains are only attainable for long residence times in the flow field, and this corresponds to stream lines that pass close to the stagnation point.[4] The presence of a stagnation point provides a region of quasi-steady-state flow (QSSF) where steady-state molecular conformations can be achieved.[12]

The optical retardation vs strain rate for a closely monodisperse poly(ethylene oxide) solution is shown in Figure 1a (solid line). A critical coil-stretch transition is indeed observed beyond $\dot{\epsilon}_c$. For flexible molecules τ is found to depend, almost universally, upon molecular weight (M) as

$$\tau \propto \eta_s M^{1.5}/(kT) \tag{2}$$

where η_s is the solvent viscosity.

The residual width of the coil-stretch transition can be ascribed to the polydispersity of the dilute solution. Indeed utilizing eq 2 we have demonstrated how it is possible to use our technique to derive the molecular weight distribution from the retardation vs strain rate curves.[4]

In this paper we describe the use of such techniques to create controlled mechanical and thermal scission and to simultaneously assess the molecular weight of the scission products.

1.1. Previous Results. As the strain rate is increased beyond $\dot{\epsilon}_c$, along the horizontal plateau in Figure 1a (solid line), the already stretched out chains become increasingly stressed until they rupture. It is then possible to stop the experiment and start again from $\dot{\epsilon} = 0$, remeasure the new I vs $\dot{\epsilon}$ curve, and derive the resultant molecular weight distribution. Thus the method can both break the chains and characterize the fracture products of the scission. It must be remembered that only a small fraction of the molecules present passes through the localized zone (i.e., birefringent line) where the chains are extended. From these chains, only a fraction are broken in a single pass; therefore, the number of unfractured molecules left diminishes gradually with the number of runs.

Odell and Keller[5] found that the fracture behavior of dilute solutions of PEO and aPS was very similar. As $\dot{\epsilon}$ is increased beyond $\dot{\epsilon}_c$, no appreciable fracture occurs until a critical fracture strain rate $\dot{\epsilon}_f$ is reached. Figure 1 shows degradation results obtained by circulating the polymer solution (a closely monodisperse PEO) at $\dot{\epsilon} > \dot{\epsilon}_f$ through a cross-slot apparatus. Figure 1a shows the raw data, and Figure 1b the derived molecular weight distribution. The latter shows the development of fracture for progressively longer times above $\dot{\epsilon}_f$. It is very clear how the initial single peak of the 1.4×10^6 M_w is gradually replaced by a second peak at 0.7×10^6 M_w.

The molecules are breaking almost precisely in half. This result has been predicted by a number of authors[2,13] and might be anticipated from the centrosymmetric nature of the flow field with respect to the molecule, resulting in a maximum stress at the chain center. These results were qualitatively explained by applying Stokes' law to a simple stretched out string of beads.[5] The predicted molecular weight dependence of the critical fracture ($\dot{\epsilon}_f$) based upon such a simple model is

$$\dot{\epsilon}_f \propto 1/M^2 \tag{3}$$

When the experiments described were repeated with a series of aPS fractions, the validity of eq 3 was strikingly verified.[4-6]

Equation 3 has a further important consequence. The critical strain rates for stretching and fracture both decrease with molecular weight; however, $\dot{\epsilon}_f$ decreases faster (proportional to M^{-2}) than $\dot{\epsilon}_c$ (proportional to $M^{-1.5}$). There will be a value of M at which $\dot{\epsilon}_f = \dot{\epsilon}_c$, indicating that at a sufficiently large M, the molecules cannot be stretched out without breaking. For aPS this value was estimated to be $M_w = 30 \times 10^6$ and again it was corroborated experimentally (see Figure 13 in ref 5).

Stokes' law can also be used to estimate the value of the actual fracture force required to break the chains. This calculation yields values that, within experimental accuracy and the known precision of the parameters involved, correspond to the force needed to break carbon–carbon bonds. One experimental result that remains unexplained by Stokes' law is the precision of chain halving with a very narrow distribution as opposed to the anticipated parabolic distribution. This result was only rationalized when the process of chain breakage was considered to be thermally activated.

1.2. The TABS Theory and Polymer Dynamics. The thermally activated barrier to scission (TABS) model is based on the assumption that the scission of backbone bonds of a linear polymer is a thermally activated process.[5,6] A brief description of the model is presented below.

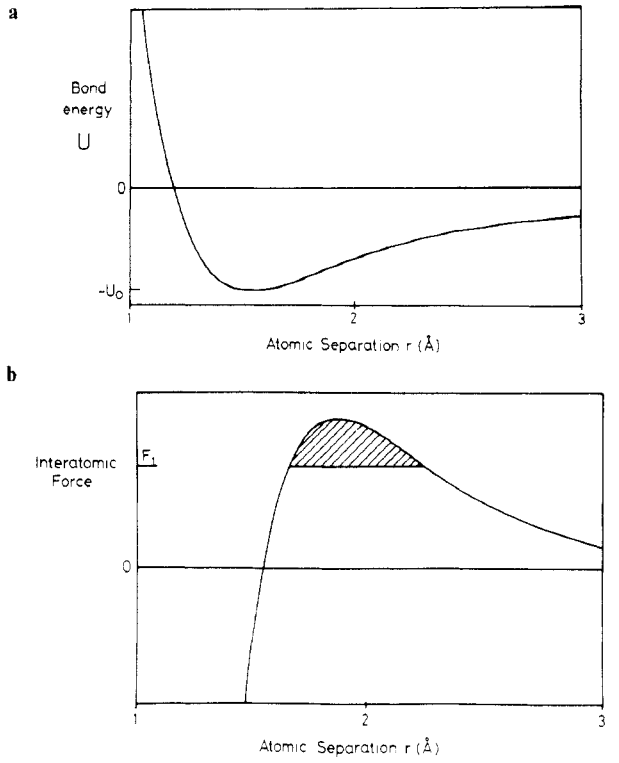

Figure 2. (a) Morse function for a covalent C–C bond. (b) Interatomic force derived from the Morse function.

First, the required force to break a C–C bond needs to be considered. The potential energy U is described as a function of the distance between two covalently bonded carbon atoms by the well-known Morse function curve of Figure 2a:

$$U = U_0(\exp[-2d(r - r_e)] - 2\exp[-d(r - r_e)]) \quad (4)$$

where r_e is the distance corresponding to the minimum in the potential energy, d the parameter defining the width of the minimum, and U_0 the dissociation energy.

Second, the breakage of bonds is assumed to be a thermally activated process where the rate is determined by an Arrhenius type equation. The activation energy is a function of the force applied to the individual C–C bond. The force can be derived as a function of extension from the Morse function and is illustrated schematically in Figure 2b. The shaded area corresponds to the activation energy for breakage if the bond supports a force F_1.

It is assumed that bond scission occurs when thermal fluctuations overcome the energy barrier for bond dissociation and that the only role of the elongational flow-induced stress in the chain is to reduce this energy barrier from its equilibrium value. This represents the basis of the TABS model.

The relation between the rate of scission (K_0) and the temperature (T) according to this model is given by

$$K_0 \propto \exp[-U_0/(kT) + (a/l)\beta N^2/8] \quad (5)$$

where β is proportional to strain rate, N is the number of monomers, a is the stretched bond length, and l is the monomer length.

The TABS model can predict rather successfully the precision of chain halving (for details of the calculations, see ref 6). Furthermore, the total scission rate can also be predicted as illustrated in Figure 3, where the width of the distribution of scission around the chain center is also shown. The total scission rate is zero below $\dot{\epsilon}_f$ (as expected) and takes off very sharply beyond $\dot{\epsilon}_f$. It should be noted that the model did not take into account

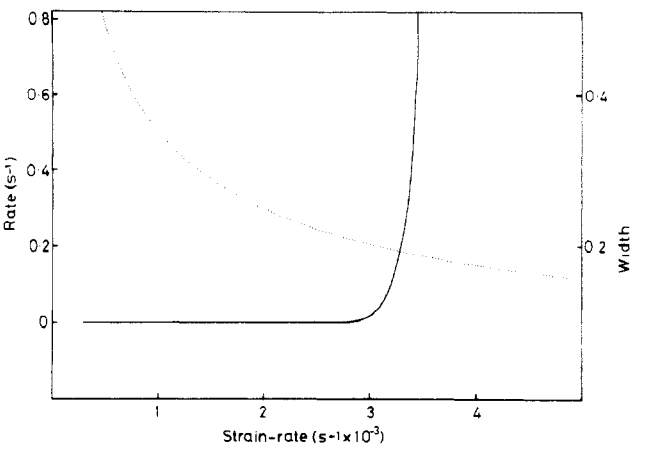

Figure 3. Total scission rate (solid line) and the width of the distribution of scission (broken line) around the chain center vs strain rate as predicted by the TABS theory for aPS (1×10^7 M_w).

the effect of the polydisperity of the polymer. The criticality observed in Figure 3 would be reduced (i.e., a broader range in $\dot{\epsilon}_f$ during the increase in scission rate) if the polydispersity is taken into account.

1.3. Objectives. Thermal stability of chains is, of course, a basic limitation to the use of polymers in general, an issue compounded with their mechanical stability in flow. Our first objective will be to examine the two effects in combination. Specifically, how far does temperature affect the breakability of the chains under flow as assessed by the single parameter of critical fracture strain rate $\dot{\epsilon}_f$. This serves as a test of our theoretical understanding (TABS theory) and as an assessment of the practical temperature limitations of elongational flow applications of polymeric additives. As part of this objective we investigate thermal degradation under static conditions, with the aid of our flow-based molecular weight characterization method.

Measuring the rate of scission (at a given temperature) as a function of strain rate ($\dot{\epsilon}$) greatly widens the single parameter approach adopted so far and is our second objective.

There exist no data on scission rates for QSSF experiments. This information is useful because it determines the lifetime of flow-modification polymers. There is, however, another reason for looking at isolated chain scission, particularly at high strain rates. This has arisen from interest in the dynamics of chain stretching.

Many real flows are not QSSF but fast transient flows (FTF) and do not possess a stagnation point (e.g., capillary entrance flows); hence, complete chain extension does not occur. FTF produces partial chain extension and therefore one would ask what the partially extended molecule looks like, what are its flow modifying effects, and perhaps most pertinently, can it break? The issue has profound conceptual implications on the mode of chain extension itself, hence on the fundamentals of chain dynamics.

Our third objective is to apply our knowledge of chain behavior in idealized elongational flow fields to chain degradation in practically occurring flow systems. As an example we have chosen to investigate the mechanism involved in the process of pore flow.

Extension of our work to more concentrated systems, where chains are entangled, is our final objective. Here some initial experiments will be reported with forward-looking implications.

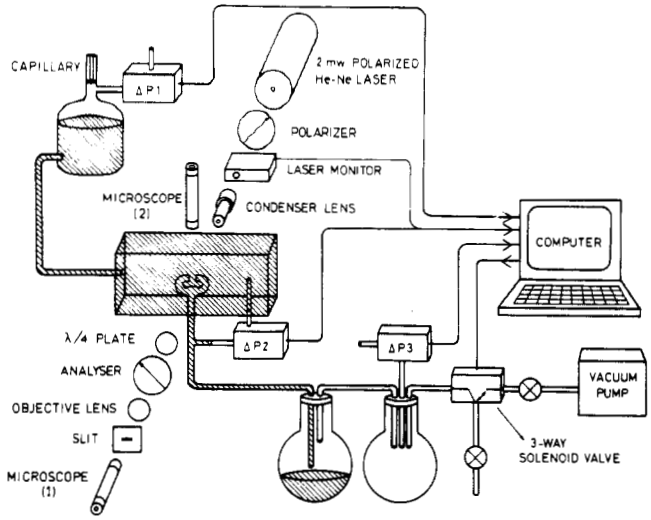

Figure 4. Schematic diagram showing the opposed-jets apparatus, associated optical train, and strain rate and viscometry control equipment.

2. Experimental Procedures

The experimentation followed the same principles as adopted in our preceding elongational-flow work in general and those on chain scission in particular. The opposed jet was adopted as a flow cell throughout, rather than the cross-slot flow cell in the previous scission works[1-3] in view of certain distinctive advantages. The jets are easier to align and to construct, and shear components are minimized by the absence of walls.

As described previously[5] the opposed-jets apparatus (Figure 4) is composed of two narrow capillary jets that face each other, immersed in polymer solution. As solution is sucked simultaneously into both jets, a strong pseudouniaxial flow field is created, with a stagnation point at the center of symmetry. The average strain rate is obtained on the assumption that the fluid elements entering the jets experience a longitudinal velocity gradient along the jets' symmetry axis in the form of uniaxial extension. $\dot{\epsilon}$ is calculated from the knowledge of the volumetric flow rate Q as follows:

$$\dot{\epsilon} = Q/(\pi r^2 s/2) \tag{6}$$

where s is the jets' separation and r the radius. Q is usually calibrated against either the pressure drop across a capillary (shown in Figure 4 and explained in detail in ref 14; see section 2.1) or the output voltage from the flow sensor (shown in Figure 5; see section 2.2). In either case, Q can be increased monotonically from zero by applying a controlled pressure in the flow system.[14]

2.1. Intensity Measurements. The optical train used to perform quantitative measurements of intensity vs strain rate has been described previously[5,14] and is shown in Figure 4. The linear detection method[15] was used to maximize the signal and reduce the background noise. Therefore, the intensity is linearly proportional to the retardation and is expressed as such in the raw data curves (for example, Figure 6).

It was very difficult to obtained reproducible traces of I vs $\dot{\epsilon}$ without introducing all the refinements of Figure 4. This was due to intensity fluctuations in the output signal. One problem was fluctuation of the output of the He–Ne laser. This was corrected by using a laser monitor device as shown in Figure 4. Furthermore, some lasers tested showed fluctuations in light polarization; this problem can be corrected if the laser monitor is placed between the polarizer and analyzer.

Another source of fluctuation was due to changes in the ambient temperature affecting several components of the optical train. This produced stringent requirements on the thermostability of the room housing the instrumentation. Even so certain specific measures proved helpful. Thus the $\lambda/4$ plates in particular can be very sensitive to temperature fluctuation: the use of special temperature-compensated zero-order type was advantageous. The lenses (especially the condenser lens, Figure 4) could also give rise to spurious background fluctuations. The diameter of the focused beam should be large enough to enclose all of the birefringent line within the peak of the Gaussian distribution of the laser beam intensity. The alignment of the jets with respect to the beam is crucial in this respect. Micropositioning equipment was used in practically all the components of Figure 4, which allowed a precision of alignment of ±5 μm.

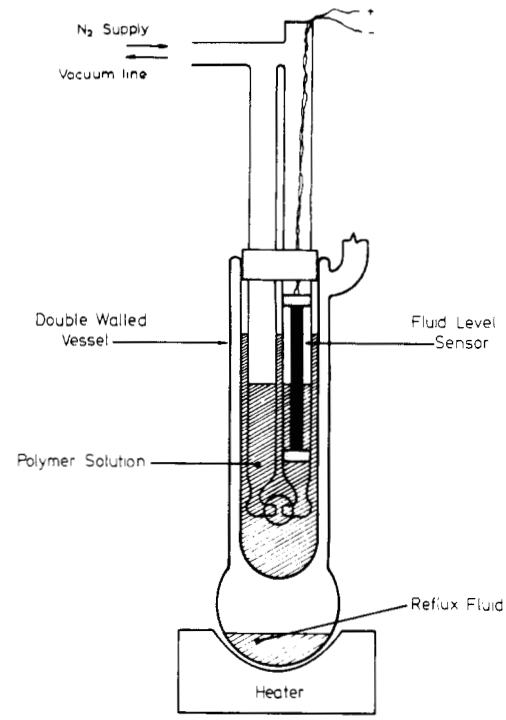

Figure 5. Modified flow cell used for high-temperature elongational flow.

2.2. Temperature-Controlled Jets. Determination of $\dot{\epsilon}_f$ as a Function of Temperature. The temperature-controlled apparatus, shown in Figure 5 is based on the opposed-jets setup, first used by Mackley.[16] This replaces the flow cell in Figure 4; the optical train remains unaltered. The jets consist of two prebored glass capillaries of 0.5-mm diameter joined to two 20-mm-diameter glass tubes that act as reservoirs. The flow rate is determined from a capacitative level sensor in the reservoir. Flow into the jets is generated by applying a vacuum to the reservoir; reverse flow is achieved by applying excess pressure of nitrogen as indicated in Figure 5. The apparatus is contained in a double-walled glass vessel with optical windows to allow the birefringence to be viewed between crossed polars. The required scission temperature (T_f) can be maintained constant by refluxing a liquid of appropriate boiling point in the outer jacket of the double-walled vessel.

The critical strain rate for chain scission at temperature T ($\dot{\epsilon}_f(T)$) was obtained by repeated passing of the solution through the jets at constant strain rates beyond $\dot{\epsilon}_c$. Only those chains that pass close to the stagnation point will be fully stretched and eventually break. Therefore a large number of runs are required to produce observable scission. After a series of tests 250 passes were found to be adequate. After degradation the retardation vs strain-rate scan was again repeated, at room temperature, to check for any indication of fracture. The latter is shown on the retardation vs strain-rate curve by a double step, or a sudden transition to a lower slope, resulting in a double peak in the derived molecular weight distribution curve. This process was repeated at progressively higher $\dot{\epsilon}$ until scission products could be observed. We estimate that we could detect degradation of 10% of the original material by this test, corresponding to 0.04% degradation per pass. This serves as our definition of $\dot{\epsilon}_f$.

In order to minimize the effects of thermal degradation, antioxidant was added to all solutions exposed to high temperatures.

2.3. Determination of Scission Rate as a Function of Strain Rate (at Room Temperature). The kinetics of degradation at a particular overstretching strain rate (i.e., at $\dot{\epsilon} > \dot{\epsilon}_f$) can be followed by measuring how the peak height in the

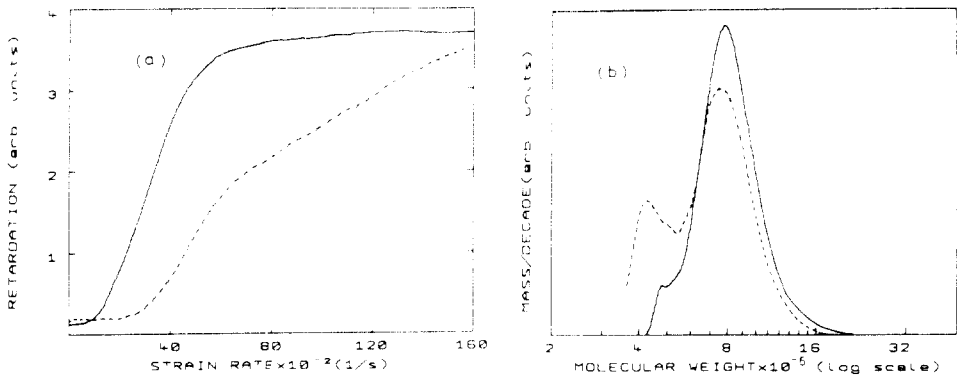

Figure 6. (a) Optical retardation vs. strain rate plots for undegraded polymer at 25 °C (continuous line) and the material degraded at 75 °C (broken line). (b) Derived molecular weight distributions corresponding to (a).

Table I
Comparison of the Molecular Weights and Polydispersities Supplied by Polymer Laboratories Ltd. and the Values Obtained with the Opposed-Jets Technique

	manufacturer's data		elongational flow	
sample	M_p	M_w/M_n	M_p	M_w/M_n
1	8×10^6	1.06	cs[a]	
2	8×10^6	1.07	8×10^6	1.07
3	7.75×10^6	<1.1	7.9×10^6	1.08
4	8.5×10^6	<1.1	8.1×10^6	1.07
5	10.5×10^6	<1.2	10.7×10^6	1.25
6	12.25×10^6	<1.3	10.7×10^6	1.2

[a] cs: sample used as calibration standard.

molecular weight distribution changes as a function of the number of degrading runs.[17] This information is contained in the retardation vs ϵ curve, which is the raw data. Therefore, the variation in the retardation value at a constant strain rate was measured as a function of the number of runs.

The strain rate chosen to measure the retardation value was ϵ_c. This was thought to be the most appropriate single parameter because it corresponds to the peak of the derived molecular weight distribution curve, while the amount of material present at twice this molecular weight or greater was usually very small (the actual value depended on the polydispersity of the sample but was always <10% for the polymers used here). The retardation is therefore proportional to the amount of remaining material of molecular weight greater than the original M_p.

In this way an absolute value of the rate of scission (i.e., the fraction of molecules passing through the jets that suffer central scission) can be obtained as a function of the strain rate. A fresh (undegraded) solution was used for each overstretching strain rate applied; then after the degrading runs, the retardation vs ϵ curve was measured at least 5 times to check for consistent results.

It is an important condition for the presently adopted evaluation of scission rate data that each chain can only be cut once even on repeated cycling. As the required ϵ_f for the fracture product is never reached within the ϵ range used, this condition is always fulfilled in our experiment.

3. Results and Discussion

3.1. Characterization of the Samples Used and Determination of Molecular Weights by Elongational Flow. Narrow fractions of aPS were used in the scission-rate determination. Before attempting to measure molecular weights, it is necessary to calibrate the instrument in order to know the numerical correspondence between molecular weight (M) and ϵ.

Six different samples were used as listed in Table I. Columns 2 and 3 give peak (M_p) and polydispersity data (M_w/M_n) as provided by the suppliers. Samples 1–4 were close to 8×10^6 M_p while samples 5 and 6 had higher M_p's. We examined all six samples by our elongational flow technique as introduced previously (e.g., ref 4) and chose concentrations for each M_p satisfying previously established criteria for dilute solution.[18]

We took sample 1, which had the lowest M_w/M_n values as specified by the supplier, as a standard and determined the M_p and M_w/M_n values of the other five samples with respect to it. Columns 4 and 5 in the table show the result. The overall agreement with the supplier is satisfactory, particularly for the samples in the 8×10^6 range, although some differences start appearing for samples 3 and 4. For the two higher molecular weight samples (samples 5 and 6) these differences become progressively larger. Throughout this work we have used our elongational flow determined values to ensure internal consistency.

At this point a comment on the potential of the elongation flow method for measuring molecular weights and their distribution is appropriate. Conventionally, GPC is used for this purpose and our suppliers' specifications were obtained in this way. However, at such high molecular weights we are at the limit of resolution of the GPC columns used, and the values quoted were obtained from the nonlinear portion of their calibration curve (Polymer Laboratories, technical booklet information). It is reasonable to assume that 8×10^6 M_p may be the upper bound for accurate GPC measurements, if low pumping rates are used (see section 3.4).

On the other hand, the elongational flow method used here does not present such problems. It is very sensitive to high molecular weights and its upper limit is determined by the molecular weight at which $\dot{\epsilon}_c = \dot{\epsilon}_f$ ($\approx 3 \times 10^7$ M_p aPS; see ref 5). It has, however, a lower limit that is determined by the maximum achievable strain rate (for aPS/Decalin solutions, it corresponds to $\approx 2 \times 10^6$ M_p using the present apparatus). In this lower range other methods to determine molecular weights are available, including GPC.

3.2. Temperature Dependence of Chain Scission. 3.2.1. Flow-Induced Scission at High Temperatures. Figure 6 illustrates the flow-induced degradation results at high temperatures. The solid line of Figure 6a shows the retardation (R) vs ϵ curve for an undegraded 8×10^6 M_p aPS; the curve corresponds to a typical coil-stretch process (similar to PEO in Figure 1), where the width of the transition is due to the residual polydispersity of the sample. The derived molecular weight distribution is shown in Figure 6b and is broadly consistent with GPC, subject to the restrictions of that technique (see section 3.4). After running until degradation is detected (in this example, the degradation temperature was 75 °C), the retardation vs strain-rate curves appear as shown in Figure 6a, with a clear shift to higher strain rates and a second slope in the retardation profile.

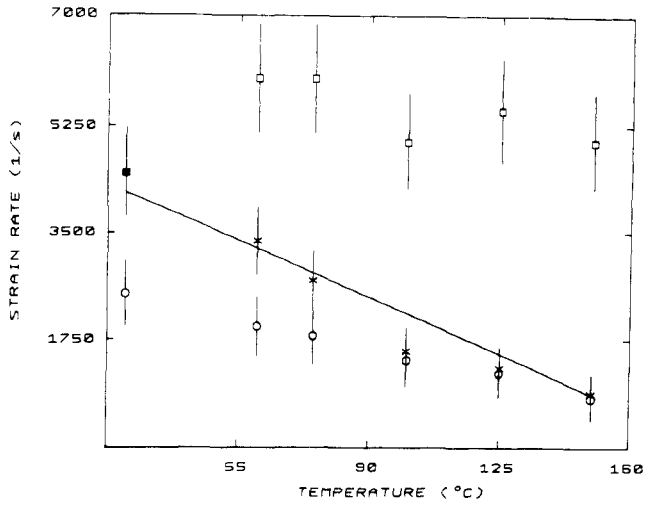

Figure 7. Critical strain rate for chain scission (ϵ_f) as a function of temperature, uncorrected (□) and corrected (×) for solvent viscosity. Also shown is the variation of critical strain rate for the coil-stretch transition (ϵ_c) as a function of temperature (○). Continuous line is the "best fit" for the TABS model.

The derived molecular weight distribution (Figure 6b), shows a narrow degraded peak arising at 4×10^6 M_p; that is, the chains are almost exactly halved (similar to Figure 1b for PEO). It is interesting to note that the position of the peak of the remaining original material is shifted toward a lower molecular weight (ca. 7.7×10^6). This arises from preferential degradation of the highest molecular weight species within the original distribution.

Figure 7 shows the variation in critical strain rate for fracture over the temperature range 25–150 °C, obtained from curves such as Figure 6. Within experimental uncertainty ϵ_f as directly determined (squares in Figure 7) is independent of temperature. However, the viscosity of the solvent (Decalin) drops by more than 80% (0.0024 Pa·s to 0.00042 Pa·s) over this temperature range. The stress transferred to the molecule is proportional to the solvent viscosity, predicting a value of ϵ_f that should be inversely proportional to solvent viscosity.[19] Therefore, we have normalized our results to a constant effective viscosity (0.0024 Pa·s). The effect of the correction is to multiply ϵ_f by η_T/η_R, where η_T is the solvent viscosity at temperature T and η_R is the viscosity at room temperature (25 °C). The corrected results are represented by crosses in Figure 7.

Also shown in Figure 7 (circles) is the critical coil-stretch strain rate (ϵ_c) as a function of temperature and corrected for changes in solvent viscosity. The solvent viscosity corrected critical strain rate for fracture now decreases markedly with temperature, approaching the critical strain rate for the coil-stretch transition at higher temperatures (Figure 7). The solid line in Figure 7 shows the prediction for ϵ_f from the TABS theory, in excellent agreement with our results. This fit is achieved with, essentially, only one adjustable parameter U_0, the dissociation energy. The value corresponding to our best fit is 172 kJ·mol^{-1}, broadly in line with values of U_0 determined from kinetics of weak-link theory of thermal degradation; for further discussion the reader is referred to ref 21 and 27.

Many useful rheological phenomena in polymer solutions, such as drag reduction, viscosity enhancement, or non-Newtonian properties, are thought to be related to the coil-stretch phenomenon occurring in extensional components of the flow field.[14,20] The utility of such applications requires that the molecules can withstand stretching without significant scission. Thus the region of flow between ϵ_c and ϵ_f is the useful "window" for coil-stretch-related phenomena. It is clear from our results that as the temperature approaches 125 °C, this window is closing, so that ϵ_f and ϵ_c are converging, setting a limit upon the useful application of polymers for flow modification at high temperatures.

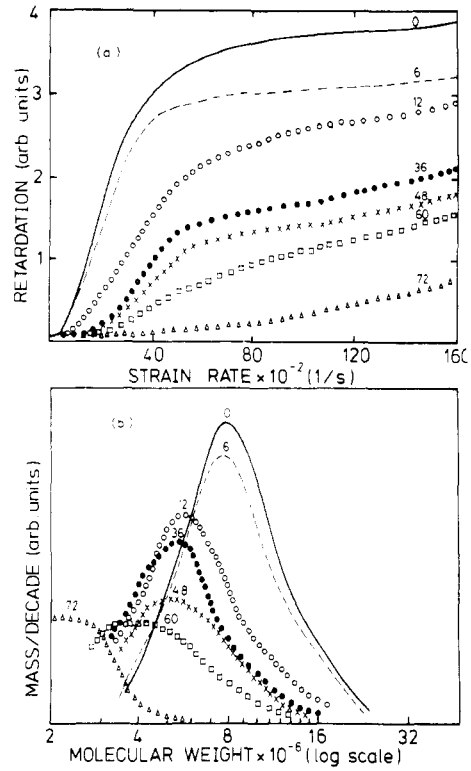

Figure 8. (a) Retardation vs strain rate plots for storage at 150 °C without flow. (b) Derived molecular weight distributions. The numbers on the curves are the storage times given in hours.

3.2.2. Pure Thermal Degradation. As the setup of Figure 5 is well suited for investigating this aspect of molecular degradation, we carried out some measurements on the same aPS/Decalin system at 150 °C in order to ascertain the extent to which thermal degradation alone, under static conditions, might affect our results. For this purpose a fresh solution containing antioxidant was stored at 150 °C without flow for up to 72 h. During the storage period the solution was cooled to room temperature at six hourly intervals to monitor the variation in retardation with strain rate.

The results show a progressive drop in the retardation vs strain rate curve as the solution is thermally degraded (Figure 8a). The derived molecular weight curve shows a corresponding reduction of the peak height, the peak position along the molecular weight axis gradually shifting toward the lower end of the scale (Figure 8b).

It is a well-known phenomenon that above a "ceiling" temperature polystyrene (and many other polymers) is unstable and degradation can lead to chain "unzipping", to leave only low molecular weight oligomers and rings.[21] In our experiments such degradation products would be far too low in molecular weight to register; they would effectively disappear from our molecular weight distribution. The consequence of this is that the maximum value of retardation oberved would be reduced. This we certainly observe. Figure 8a shows that the maximum retardation is drastically reduced by prolonged thermal degradation at 150 °C; this may be contrasted with Figure 6a, where the degradation is principally mechanical

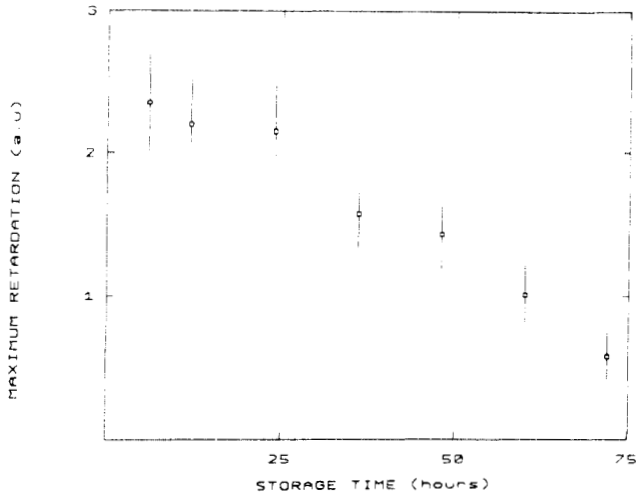

Figure 9. Maximum retardation from Figure 8 as a function of storage time at 150 °C.

and almost no reduction in maximum retardation is observed. While the ceiling temperature for aPS melts is ca. 395 °C, there is evidence that unzipping can occur at temperatures as low as 150 °C in solution.[58]

Figure 9 shows the maximum retardation at 150 °C as a function of time. After 25 h it appears that the rate of unzipping accelerates; it may be that the antioxidant is becoming exhausted.

The results of Figure 8 show that the thermal degradation, without any mechanical fracture, does not yield the central scission that typifies flow-induced degradation. Instead each curve displays typical random scission behavior with concomitant broadening of the molecular weight distribution. The initial degradation half-life of 24 h is broadly consistent with predictions of TABS theory, which predicts a half-life of 34 h.

Gel permeation chromatography is an appropriate technique for examining the lowest molecular weight scission products. Results obtained are broadly consistent with the degradation results based on extensional flow and confirm the existence of substantial material of $<2 \times 10^6$ molecular weight at long degradation times.

3.2.3. Combined Flow-Induced and Thermal Degradation. Figure 10 shows the combined effect of flow-induced and thermal degradation. In this case, the polymer solution was first mechanically degraded, as before, for only 250 passes (6 h) at 150 °C and then stored at this temperature, and the changes in optical retardation with strain rate were monitored at six hourly intervals (Figure 10a).

The derived molecular weight distributions shown in Figure 10b again reveal all the effects associated with both types of degradation. First, the double peaks indicate (as in Figure 6b) midchain scission associated with flow-induced degradation. Second, we see the drop in retardation and the broadening of the molecular weight distribution, which by the previous section (Figure 8) we can now attribute to thermal degradation. Finally, the shifting of the peaks toward the lower end of the molecular weight scale, as explained previously, arises from preferential degradation of the highest molecular weight species.

3.3. Scission Kinetics and Implications for the Dynamics of Chain Stretching. As indicated under objectives (section 1.3) the kinetics of chain scission have important implications for chain dynamics. We shall now discuss this subject in more detail.

3.3.1. Models of Chain Dynamics. One attractive model for the dynamics of chain stretching is the so-called

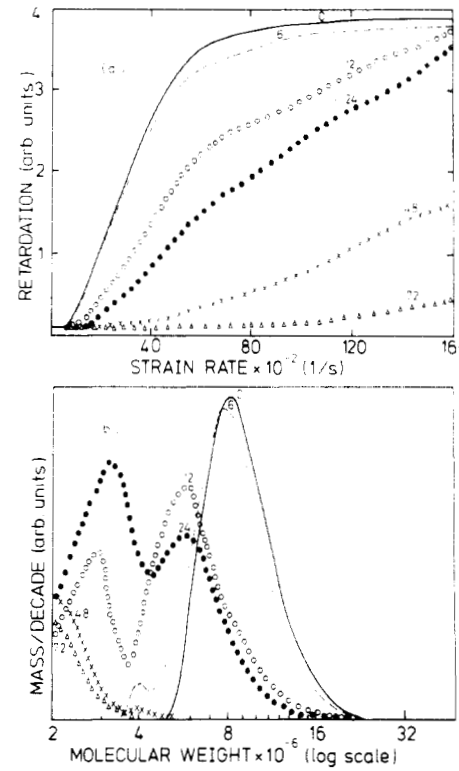

Figure 10. Combined effects of flow for 250 passes at 150 °C followed by storage at 150 °C. (a) Retardation vs strain rate. (b) Derived molecular weight distributions.

"yo-yo" model due to Ryskin.[22] The Ryskin model was motivated by the description of the terminal equilibrium configuration of a macromolecule stretched by a strong flow, first given by Frenkel.[2] Frenkel envisaged the central portion of such a molecule as being straightened out along the direction of the flow, while the two end portions remained curled.

Ryskin's yo-yo model considers that if $\dot{\epsilon} > \dot{\epsilon}_c$, the elongation of the chain in an extensional flow reflects the elongation of the fluid element. The macromolecule does not, however, deform affinely with the fluid, but unravels, whereby the central portion of the molecule is straightened out first and then remains taut and grows in length at the expense of the two coiled end portions. These end portions move apart under the influence of the flow while at the same time getting smaller. The reason for such behavior, according to Ryskin, is the nonuniform distribution of the stretching force along the hydrodynamically effective length of the molecule. The stretching force is zero at the ends and maximum in the middle with a roughly parabolic distribution. If the chain enters a region of weak flow, the chain will curl back into a coil; hence each half of the chain behaves as a yo-yo.

Rabin[12] has calculated the response of such a molecule to a transient extensional flow, specifically addressing the question of whether the stress in the central portion of the chain could be sufficient for scission before the chain is predominantly extended. This he has claimed can occur if the strain rate is high enough; he predicts a scaling law of critical strain rate

$$\dot{\epsilon}_f \propto M^{-1.1} \tag{7}$$

This was roughly in agreement with some results on degradation in transient capillary flows[23] but is in contrast to the scaling law

$$\dot{\epsilon} \propto M^{-2} \tag{8}$$

observed for QSSF (stagnation point) flow in this

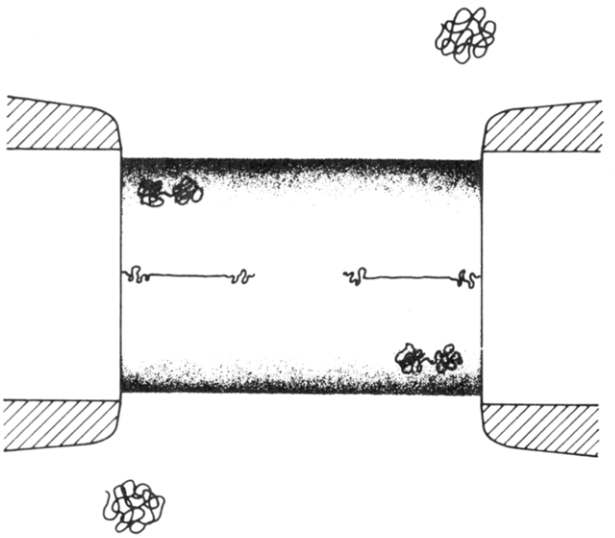

Figure 11. Schematic representation of the yo-yo model in the opposed jets. The density of dots is inversely proportional to the residence time in the flow field. The undotted central region corresponds to QSSF, and the dotted region that surrounds it corresponds to FTF. See text.

laboratory[3,5] and expected for highly stretched molecules. Rabin predicted that FTF scission would occur mostly at much higher strain rates than QSSF scission, that the strains of the molecules would be modest (≈3×), that the scission rates would be high, and that the scission would be somewhat less precisely central.

3.3.2. FTF Degradation Results. Nguyen and Kausch have performed a series of experiments using transient elongational flow. Their apparatus is essentially similar to the device described by Merrill and Leopairat.[24] The FTF is created by forcing the fluid through a steep contraction with a piston.[25] They first obtained the molecular weight dependence of $\dot{\epsilon}_f$ using bisphenol A polycarbonate[26] and then aPS.[27] Their first two works reported a molecular weight dependence of $\dot{\epsilon}_f$ in agreement with the QSSF result (i.e., $\dot{\epsilon}_f \propto M^{-2}$). They later reconsidered their strain-rate calculations and obtained a different scaling law, $\dot{\epsilon}_f \propto M^{-0.95}$.[28] These new results were in agreement with Merrill's unpublished results on FTF ($\dot{\epsilon}_f \propto M^{-1.1}$ [23]) and were rationalized in terms of the Rabin model, with which it thus seemed to agree except for the very precise halving of the chain, a feature still displayed by these experiments.

Recently, Nguyen and Kausch have investigated the effect of solvent viscosity on their FTF results.[29] Surprisingly, they found that $\dot{\epsilon}_f$ is almost independent of solvent viscosity. A small reduction in $\dot{\epsilon}_f$ was found only for very viscous solvents. This result goes against the fundamental predictions of any molecular model of polymer dynamics. A viscous solvent will increase the stress on the molecules and it will increase the molecular relaxation time by a factor proportional to the solvent viscosity. Such a fundamental consideration is independent of the mechanism of chain unraveling and fracture.

3.3.3. Scission-Rate Results and Their Interpretation in QSSF. One of the problems of the Rabin model is that it would predict that below a certain molecular weight, scission would occur in a FTF earlier than in a QSSF of the same strain rate (because of the reduced power dependence of $\dot{\epsilon}_f$ upon M as compared to QSSF). This is clearly not a satisfactory situation, since a QSSF necessarily incorporates a FTF at its inception and at all points surrounding the stagnation point. Figure 11 presents a schematic diagram of the opposed jets showing

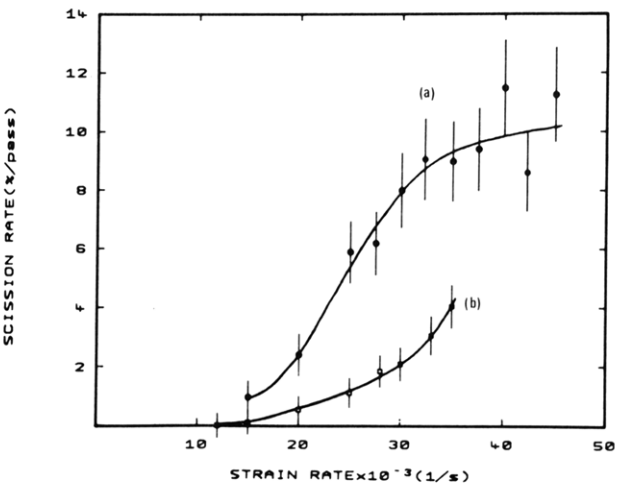

Figure 12. Scission rate vs overstretching strain rate for dilute solutions of aPS in Decalin at room temperature: (a) M_p = 10.7×10^6, M_w/M_n = 1.2, 0.01%. (b) $M_p = 8.1 \times 10^6$, M_w/M_n = 1.07, 0.02%.

the regions of FTF and QSSF and also a sketch of how the molecules would deform in these regimes according to the yo-yo model.

Our experiments on scission rate vs strain rate can also probe the region of strain rates where "transient" scission should dominate. The flow field of Figure 11 consists of a very restricted region of QSSF (long residence time) around the stagnation point. This is surrounded by a region of FTF (lower strain, short residence time; dotted regions in Figure 11). Normally, the observed birefringence corresponds to highly stretched chains only in the QSSF region, i.e., localization. On the prediction of the Rabin theory and Nguyen and Kausch experiments, at high strain rates transient chain scission in the "yo-yo" configuration should produce a massive increase in scission rate. This arises because the yo-yo model only requires low strains for scission, such that almost every molecule passing through the jets would break. The results obtained here show clearly this is not the case.

Figure 12a shows the results of scission rate as a function of overstretching strain rate for 10.7×10^6 M_p narrow aPS fraction. It is important to note that in order to break the chains, the polymer solution must be overstretched at strain rates that are much higher than $\dot{\epsilon}_c$. At these strain rates the birefringent line width has already achieve its maximum value. For instance, for the 10.7×10^6 M_p aPS the maximum line width was observed at ≈5200 s^{-1}.

In order to compare the results presented here with those obtained by FTF, the corresponding fracture or overstretching strain rates must be used. Nguyen and Kausch have produced such results for four different M_w aPS fractions; unfortunately, their maximum M_w was lower than ours (2.86×10^6). Nevertheless, their curve of log $\dot{\epsilon}_f$ vs log M (Figure 7 in ref 28) can be extrapolated to 10.7×10^6 M_p, yielding a value of 7000 s^{-1}. At this strain rate there is virtually no degradation in the opposed jets (Figure 12a). As the strain rate is increased in Figure 12a, the scission rate gradually increases, but there is saturation beyond ca. 30 000 s^{-1}, the scission rate still corresponding to only ≈10% of the molecules passing through the jets. This is equivalent to the proportion of molecules that are highly stretched, as judged by the width of the birefringent line and the known flow field. The maximum width of the birefringent line was 100 ± 10 μm, to be compared with the jets' diameter, 350 μm. Allowing for this we arrive at the important conclusion that

at the saturation strain rate all the chains that pass through the active portion of the flow field (as represented by the birefringent line) break. It follows that only highly stretched out chains can suffer scission. This is in direct contradiction with the prediction of scission of partially stretched chains envisaged by the Rabin theory as applied to the Ryskin model and supported by the Nguyen and Kausch experiment.

The molecular weight dependence of scission provides further support for the above conclusion. While our test for this in the present scission-rate determination is only fragmentary, it suffices for the point to be made.

Figure 12b shows a corresponding curve for 8.1×10^6 M_p aPS. The curve is shifted to higher strain rates; even though it does not saturate within the range of strain rates used, the maximum rate of scission (4.2%) is far less than would be expected for transient scission.

If the curves of Figure 12 are compared with the TABS prediction of Figure 3, a qualitative agreement is observed although a substantial broadening of the experimental scission-rate curve is evident. The spread of scission strain rates (i.e., beyond the spread intrinsic to a monodisperse polymer (Figure 3)) reflects the polydispersity of the polymer samples. In analogy with our previous practice in defining $\dot{\epsilon}_c$, we shall take $\dot{\epsilon}_f$ as corresponding to the peak of the molecular weight distribution. Therefore, $\dot{\epsilon}_f$ (used as a single parameter so far) should correspond to the strain rate at the steepest part of the curve and not the first $\dot{\epsilon}$ at which fracture is observed (which should correspond to the strain rate needed to break the longest molecules of the molecular weight distribution).

Having defined $\dot{\epsilon}_f$ in terms of fracture strain rates, we are in a position to extract the molecular weight dependence of scission rates. If such scission rate values are extracted from Figure 12 for the two aPS fractions used ($\dot{\epsilon}_f \approx 16\,000\ s^{-1}$ for the 10.7×10^6 M_p aPS and $\dot{\epsilon}_f \approx 28\,000\ s^{-1}$ for the 8.1×10^6 M_p aPS), a scaling law of $\dot{\epsilon}_f \propto M^{-2.01}$ is obtained, in agreement with previous results on the cross-slot apparatus.[5] It should be noted that this criterion for $\dot{\epsilon}_f$ is distinct from the working definition used for thermal studies (section 2.2), where the detailed dependence of scission rate upon strain rate has not been determined, and is also distinct from that in our earlier works on scission.[5] Thus we see that the molecular weight dependence of scission, while corroborating our previous findings, is at variance with predictions from the yo-yo model and the Nguyen–Kausch experiments that appear to have supported it.

It is a prediction of the Ryskin model that when a molecule is unraveling, the taut central portion generates a large additional stress via a dissipative mechanism. The yo-yo model thus predicts a very large viscosity increase during the transient stretching as opposed to any other model of polymer dynamics. The classical models of Peterlin[9] and de Gennes[11] predict that a large stress is only produced when the macromolecule is stretched to ca. 90% of its contour length.

Previous results of extensional viscosity measurements generally support the classical theories and not the yo-yo model.[18] According to Ryskin, an effective viscosity increase of 2 orders of magnitude may be expected during FTF. However, the increase in effective extensional viscosity observed previously[18] correlated very well with the appearance of the coil-stretch transition. There was no viscosity effect below $\dot{\epsilon}_c$, and above $\dot{\epsilon}_c$ the magnitude of the effect could only be accounted for by the classical type models applied only to those molecules that could be seen to be highly stretched (i.e., the birefringent line).

In summary, the results of this section, namely the saturation of the scission rate, the observed molecular weight dependence of the scission, and the qualitative trend in viscosity invoked from our previous works, all indicate that unless the molecules are fully stretched out by the flow field, chain scission will not occur. We consider this conclusion of significance not only for our understanding of the scission process but also for that of the underlying dynamics of chain stretching. There remains to account for the apparent conflict with existing FTF results.

3.3.4. Possible Origin of Conflict with Results in FTF. The FTF results quoted in section 3.3.1 leave no doubt that the chains break very precisely in the center. The problem is very complex and there is no definite solution yet; nevertheless two possible ways of explaining the results are presented below.

One possible mechanism that can explain the central scission observed by Merrill and Nguyen and Kausch in FTF is based upon flow modification. It is well-known that even minute quantities of polymer additives can modify the Newtonian flow field in capillary entrance flows or flow through contractions.[20] In the FTF experiments of Merrill and Nguyen and Kausch, it is argued that the molecules accelerate toward the orifice in a very short distance (of the order of the diameter of the orifice), and therefore the chains do not have time to accumulate the strain required to unravel. However, if the flow field is modified by the addition of the polymer, the point from which the molecules accelerate can be pushed further away from the entrance of the orifice, and the chains would have more time to experience the high $\dot{\epsilon}$. Flow visualization experiments have shown that such flow-modifying effects persist to very small concentrations in polyacrylamide/water solutions.[30] The total strain available in FTF is nevertheless limited by the geometry of the contraction. The strain rate required to break the highest molecular weight fractions will be higher if the strain is limited than if the strain is infinite (QSSF) because the molecules do not deform affinely with the fluid. Therefore, for a limited constant strain, the value of the power law exponent will be reduced. Such a power law in a FTF experiment should be a function of the total available strain. This problem does not arise in QSSF because of the presence of the stagnation point, which offers very high strains to the molecules that pass close to it.

An alternative explanation for the FTF results can be given if the flow field produced after the fluid has left the orifice is turbulent. In the experiments of Nguyen and Kausch, the fluid is pushed through a 0.5-mm orifice from a cylindrical reservoir of 21.3-mm diameter into a conical cavity. With a maximum pressure of 200 atm to push the fluid through, it would not be surprising if turbulent flow is generated in the exit cavity. It is well-known that turbulent flow induces chain halving in dilute polymer solutions,[31] but it also has been recognized that high molecular weight polymeric additives reduce turbulence. This reduction in turbulence at high molecular weights may also imply that higher strain rates will be required to produce turbulence (and hence fracture) for high molecular weight fractions. In this way, the reduction in the power law exponent could again be explained. Furthermore, turbulence might also account for the independence of $\dot{\epsilon}_f$ on solvent viscosity. An increase in solvent viscosity would increase the viscous pull on the molecules and therefore decrease $\dot{\epsilon}_f$. The use of higher viscosity solvents will, however, tend to delay the onset of

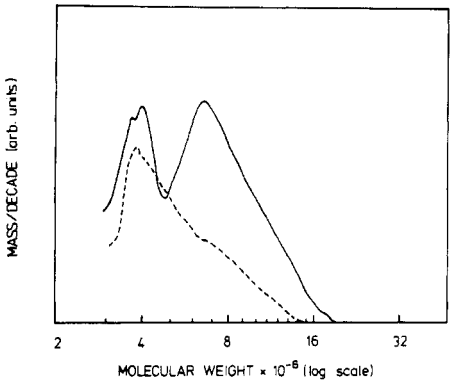

Figure 13. Molecular weight distribution curves of a 0.02% aPS solution in Decalin degraded during flow through (a) a GPC precolumn frit (solid line) and (b) a GPC column (dashed line).

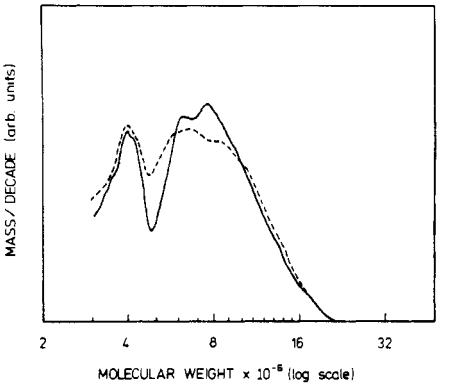

Figure 14. Molecular weight distribution curves of aPS/Decalin solutions degraded during flow through the jets at (a) 0.30% (solid line) and (b) 0.35% (dashed line). See text.

turbulence, i.e., increase the apparent value of $\dot{\epsilon}_f$. Therefore the two factors, stress on the molecules and turbulence, have opposite effects on $\dot{\epsilon}_f$ and may possibly cancel out.

3.4. Degradation of Dilute Solutions in Porous Media. The opposed-jets system offers the advantage of a well-defined idealized elongational flow field. This has been used as a basic step toward understanding more complex flows, for instance, pore flow. Pore flows arise in a wide range of practical flow situations. These include filtration and tertiary oil recovery in porous rocks. Here we chose flow in the GPC apparatus as this, being associated with molecular weight determination, has arisen naturally in the course of the present work. Initially GPC precolumn frits were used on their own and then the entire GPC columns.

Figure 13a shows the molecular weight distribution curve measured by our elongational flow method in a dilute aPS solution (0.02% aPS/Decalin, 8.1 × 10^6 M_p, originally similar to that shown in Figure 6) after is was pumped through a precolumn frit. Precolumn frits are composed of sintered stainless steel beads used to filter the solution before it enters the column and sometimes also to hold the gel beads tightly packed inside the column. At the flow rate used to pump the solution through the frit, 1.5 mL/min, chain halving occurred as evidenced by the double peak in Figure 13a. The solution suffered ≈48% degradation in just one pass.

Furthermore, if another virgin solution is pumped through a GPC column (10^7 Å, supplied by Polymer Laboratories Ltd.) at the same flow rate of 1.5 mL/min, almost all of the original 8.1 × 10^6 M_p material was fractured with the peak of the distribution now centered around 4 × 10^6.

Polyisobutylene,[32] polybutadiene,[33] and aPS[34,35] have also been reported to degrade during GPC runs. The latter also showed a twofold factor decrease in M_w, but this was attributed to shear degradation by these authors. It is proposed that the highly elongational character of the pore flow is responsible for stretching and breaking the molecules in half, in a very similar process to the idealized elongational flow experiments.

In view of the results presented here, the use of GPC of determining molecular weights above an upper limit, or when there is a high molecular weight tail in the distribution curve, may be invalid for conventionally prescribed flow rates. The upper molecular weight limit will be determined by the column (precolumn frits, bead and pore size, packing characteristics, etc.) and the flow rate used. The influence of these variables is presently being studied.

3.5. Degradation of Semidilute Solutions: Some Initial Experiments. While as far as the present authors are aware there are no data on the concentration dependence of scission rate in idealized elongational flow experiments, one would reasonably anticipate marked differences in the degradation behavior of stretched interacting molecules. The most obvious expectation would be the disappearance of preferential breaking near the center of the molecule as higher concentrations are approached.

In the idealized elongational flow experiments conducted so far, we found no concentration dependence in dilute solutions of 8.1 × 10^6 M_p aPS in Decalin in the concentration range 0.0075–0.025%. This was anticipated on the basis of negligible entanglement effects. At higher concentrations the scission rate was found to increase with concentration. Such a positive concentration dependence can be rationalized in terms of the increased entanglement effects and molecular stresses evidenced by elongational viscometry.[18]

Two results will be presented here in the semidilute range of 8.1 × 10^6 M_p aPS. They correspond to the maximum concentrations explored so far, 0.3% and 0.35%. Both solutions were degraded by repeated running through the jets at $\dot{\epsilon} \approx 18\,000\ s^{-1}$. Then both solutions were diluted to 0.02% in order to determined their molecular weight distribution after degradation. Figure 14 presents the molecular weight distribution of the degraded solutions, which should be compared with the undegraded solution shown in Figure 6b.

As can be seen in Figure 14 both solutions still show central scission, contrary to the expectations mentioned above. Nevertheless, Figure 14b (the more concentrated solution) shows a less pronounced dip between the two main peaks which might indicate a more randomized scission than in the 0.3% solution (solid line in Figure 14) or in the dilute case (Figure 6b). Clearly, the concentration differences are too small for any conclusion to be drawn; nevertheless they may be pointers in the anticipated direction which are being followed up presently.

The scission rate for both semidilute solutions was found to be much higher than that for the corresponding dilute solution. The scission rate was 1.1%/run for the 0.3% solution and 1.5%/run for the 0.35% solution, which are almost 3 and 4 times higher, respectively, than the scission rate of the dilute solution at the same overstretching strain rate (0.4%/run; see Figure 12 (curve b) at 18 000 s^{-1}). This result corroborates the previous but more qualitative findings of increasing scission rate with concentration in PEO,[36] HPAA,[14] and aPS.[18] Furthermore, the solution concentration in both solutions was high enough

to show entanglement formation together with strong non-Newtonian effects as evidenced by flow-resistance measurements.[18] On the other hand, it has been found that in the case of monodisperse aPS the entanglements that evolve with increasing $\dot{\epsilon}$ induce a breakdown of the flow field, annihilating the stagnation point.[18] The initially QSSF flow field thus becomes transient (FTF), which should be less effective in breaking molecules. This being so, it might not be possible to obtain a randomized scission as expected, unless the number of entanglements per chain is greatly increased. Experiments with such highly concentrated solutions of monodisperse aPS are in progress.

3.6. Chain Scission in Simple Shear Flow. Most past studies on flow degradation (other than those reviewed in section 3.3.2) have been carried out in simple shear flows. Even in simple shear flow there is not conclusive evidence regarding the concentration dependence of degradation. Conflicting data exist in the literature; some authors suggest that the scission rate increases with increasing polymer concentration,[37-39] while others suggest that it is independent of concentration.[40-44] A negative concentration dependence (i.e., decrease in scission rate with increasing concentration) is also often found in the literature[45-48] as well as complex functions of the concentration.[49-51] This is partly due to the nature of shear degradation experiments, where often complex flow fields and ill-defined experimental conditions are used.

The majority of the works that claimed to have found shear flow degradation used high-speed stirring, capillary flow at very high flow rates, or high-shear concentric cylinder viscometers. These experiments most probably involve turbulent flow with its concomitant high elongational component. In most experiments the authors claimed to have worked under laminar conditions on the basis of low Reynolds number calculations but without taking into account the effect of the polymers on the flow field, which have been seen to induce or suppress flow instabilities and turbulence.[18]

Simple shear flow is composed of pure shear and rotation.[52] Therefore, in shear flow, before the chain is greatly extended it has rotated into a position in which the flow is reversing that extension.[52] Although some birefringence can be observed in simple shear flow (conventional flow birefringence experiments), it is always small even at high shear rates.

In dilute solution there appear to be no theoretical reasons to expect degradation in simple shear flows. Cerf[53] has calculated the molecular shape of a randomly coiled molecule in a shear flow field based on the dumbbell theory. The molecular shape reaches a steady state represented by an ellipse with the principal axes of deformation rotated away from the direction of elongational rate by an angle $\theta \approx \gamma\tau$ that approaches $\pi/4$ for higher values of shear rate. Lumley[54] has calculated that the expansion of the coil diameter in a two-dimensional shear flow is restricted and therefore, bond scission should not occur. Other factors that could prevent the coil from being stretched, such as internal viscosity, steric shielding, and decreasing frictional contact with the solvent, will further hinder the degradation effect.

In view of these theoretical considerations, it is difficult to envisage how a simple laminar shear flow can cause chain scission in dilute solutions. Indeed experiments that have been performed with due attention to the onset of turbulence in capillary flow have confirmed that no shear degradation can be observed in unentangled solutions (dilute) before turbulent flow sets in.[55]

In shear flows, a negative concentration dependence has been found in many high-speed-stirring experiments. If turbulence is causing the chain fracture observed, increasing the polymer concentration can reduce or delay the onset of turbulence, and a negative concentration dependence may be expected. Some authors[39] have argued that the true concentration dependence of scission rate should be positive in shear flows, also on the basis of intramolecular entanglements being increased with increasing concentration. However, the common theoretical argument that is used to explain such positive concentration dependence in shear flows is based on the stress concentration buildup at the points of physical junction, often invoked in rubber elasticity theory.[56] This treatment, however, may be inadequate to described the entanglements present in semidilute solutions where the overlap density is not as high as in a rubber and where the entanglements are transient in nature. Ballauff and Wolff[39] claimed that their high-shear concentric cylinder viscometer produces a laminar flow field, because the maximum Reynolds number used was 10 and the maximum Taylor number 1.6 (the Taylor number should be less than 41 in order to avoid Taylor vortices between the cylinders). They did not, however, visualize the flow field or perform any checks on the stability of the flow. Other results have shown the development of flow instabilities at very low Reynolds number ($Re \approx 0.07$).[57]

In summary, it is difficult to form a unified picture of chain degradtion in simple shear flow, the prevalent material on the subject of flow-induced scission in the literature. From our own background it appears that whenever scission is reported, turbulence or entanglements are likely to be involved.

4. Conclusions

We have presented results of the combined effects of flow and temperature upon macromolecular degradation in solution. We examined scission of atactic polystyrene in elongational flow fields at temperatures up to 150 °C. The scission occurs beyond a critical strain rate ($\dot{\epsilon}_f$), predominantly at the chain center. It is clear that mechanical scission plays the dominant role up to 150 °C. After correction for changes in solvent viscosity $\dot{\epsilon}_f$ is, however, found to be a decreasing function of temperature and is well modeled by the TABS theory. In the absence of flow we confirm random scission of the molecules, with a scission rate in line with expectations from theory.

The results obtained on scission rates (performed at ambient temperature) indicate that central scission in an extensional flow field occurs only for highly stretched chains (up to the maximum strain rates explored). This information has implications for the modeling of chain-stretching dynamics. It is also of potential practical importance. Nearly all flows where polymers are added for hydrodynamic effect are partly elongational in character. The performance of such polymers in providing enhanced flow resistance in porous media, antimisting effects, or drag reduction relies on the stability of the highest molecular weight components. The technique used here provides a new approach to assess this stability in a molecular weight range not easily accessible to conventional techniques. Chain scission of similar nature to that occurring in idealized extensional flows can occur in transient flows such as porous media and even GPC columns.

The scission rate in elongational flow was found to be independent of concentration in dilute solutions. For semidilute solutions the scission rate was found to increase

with concentration. These findings were compared with results obtained in shear flows where the experimental conditions used could produce high elongational components. It is speculated that simple laminar shear flows may not be capable of degrading polymer solutions and that degradation is only encountered when the flow contains an appreciable elongational component.

Acknowledgment. We are pleased to acknowledge support from the Venture Research Unit of BP International. K.A.N. acknowledges with gratitude the financial support of the Science and Engineering Research Council. We are also indebted to Dr. T. Q. Nguyen for helpful discussion and early disclosure of his results.

References and Notes

(1) Kuhn, W. *Kolloid-Z.* **1934**, *68*, 2. Kuhn, W.; Kuhn, H. *Helv. Chim. Acta* **1944**, *27*, 493.
(2) Frenkel, J. *Acta Physicochim. URSS* **1944**, *19*, 51.
(3) Odell, J. A.; Keller, A.; Miles, M. J. *Polym. Commun.* **1983**, *24*, 7.
(4) Keller, A.; Odell, J. A. *Colloid Polym. Sci.* **1985**, *263*, 181.
(5) Odell, J. A.; Keller, A. *J. Polym. Sci., Polym. Phys. Ed.* **1986**, *24*, 1889.
(6) Odell, J. A.; Keller, A.; Rabin, Y. *J. Chem. Phys.* **1988**, *88*, 4022.
(7) Muller, A.; Odell, J. A.; Keller, A. *Polym. Commun.* **1989**, *30*, 297.
(8) Narh, K. A.; Odell, J. A.; Muller, A. J.; Keller, A. *Polym. Commun.* **1990**, *31*, 1.
(9) Peterlin, A. *Pure Appl. Chem.* **1966**, *12*, 563.
(10) Hinch, E. J. *Proc. Colloq. Int. CRNS*, **1974**, 233, 241.
(11) De Gennes, P.-G. *J. Chem. Phys.* **1974**, *60*, 5030.
(12) Rabin, Y. *J. Chem. Phys.* **1987**, *86*, 5215. Rabin, Y. *J. Non-Newtonian Fluid Mech.* **1988**, *30*, 119.
(13) Harrington, R. E.; Zimm, B. H. *J. Phys. Chem.* **1965**, *69*, 161.
(14) Odell, J. A.; Muller, A. J.; Keller, A. **Polymer 1988**, *29*, 1179.
(15) Riddiford, C. L.; Jerrard, H. G. *J. Phys. D, Appl. Phys.* **1970**, *3*, 1314.
(16) Mackley, M. R.; Keller, A. *Philos. Trans. R. Soc. London* **1975**, *A278*, 29.
(17) Basedow, A. M.; Ebert, K. H. *Adv. Polym. Sci.* **1977**, *22*, 83.
(18) Muller, A. J.; Odell, J. A.; Keller, A. *J. Non-Newtonian Fluid Mech.* **1988**, *30*, 99.
(19) Zimm, B. H. *J. Chem. Phys.* **1956**, *24*, 269.
(20) Gampert, B., Ed. *Proceedings of the IUTAM Symposium: The Influence of Polymer Additives on Velocity and Temperture Fields*; Springer: Berlin, 1985.
(21) Grassie, N.; Scott, G. *Polymer Degradation and Stabilization*; Cambridge University Press: Cambridge, 1985.
(22) Ryskin, G. *J. Fluid Mech.* **1987**, *178*, 423.
(23) Merrill, E. W. Proceedings of the American Chemical Society Meeting in Chicago, Sept 1985; private communication to Y. Rabin.
(24) Merrill, E. W.; Leopairat, P. *Polym. Eng. Sci.* **1980**, *20*, 505.
(25) Nguyen, T. Q.; Kausch, H. H. *Colloid Polym. Sci.* **1986**, *264*, 764.
(26) Nguyen, T. Q.; Kausch, H. H. *Polym. Prep. (Am. Chem. Soc., Div. Polym. Chem.)* **1987**, *28*, 409.
(27) Nguyen, T. Q.; Kausch, H. H. Presented at the American Chemical Society Meeting in New Orleans, Division of Polymer Chemistry, Sept 1987. Also commented on by H. H. Kausch in: *Polymer Fracture*, 2nd ed.; Springer: Berlin, 1987.
(28) Nguyen, T. Q.; Kausch, H. H. *J. Non-Newtonian Fluid Mech.* **1988**, *30*, 125.
(29) Nguyen, T. Q. private communication, 1989.
(30) Sellin, R. private communication, 1988.
(31) Merrill, E. W.; Horn, A. F. *Polym. Commun.* **1984**, *25*, 144.
(32) Huber, C.; Lederer, K. H. *J. Polym. Sci., Polym. Lett.* **1980**, *18*, 535.
(33) Fulton, S., private communication, 1989.
(34) Slagowski, E. L.; Fetters, L. J.; McIntyre, D. *Macromolecules* **1974**, *7*, 395.
(35) McIntire, A. L.; Shih, J.; Savoca, R.; Seeger, R.; MacArthur, A. In *ACS Symp. Ser.* **1984**, *No. 245*, 227.
(36) Keller, A.; Muller, A. J.; Odell, J. A. *Prog. Colloid Polym. Sci.* **1987**, *75*, 179.
(37) Rodriguez, F.; Winding, C. C. *Ind. Eng. Chem.* **1959**, *51*, 1281.
(38) Shimada, T.; Horng, P. L.; Porter, R. S. *J. Rheol.* **1980**, *24*, 783.
(39) Ballauff, M.; Wolff, B. A. *Adv. Polym. Sci.* **1988**, *85*, 1.
(40) Johnson, W. R.; Price, C. C. *J. Polym. Sci.* **1960**, *45*, 217.
(41) Minoura, Y; Kasuya, T.; Kawamura, S.; Nakano, A. *J. Polym. Sci., Part A-2* **1967**, *5*, 125.
(42) Nakano, A.; Minoura, Y. *J. Appl. Polym. Sci.* **1971**, *15*, 927.
(43) Abdel-Alim, A. H.; Hamielec, A. E. *J. Appl. Polym. Sci.* **1973**, *17*, 3769.
(44) Kaverina, N. I. *J. Appl. Chem. USSR (Engl. Transl.)* **1956**, *29*, 1565.
(45) Porter, R. S.; Johnson, J. F. *J. Appl. Phys.* **1964**, *35*, 3149.
(46) Ram, A.; Kadim, A. *J. Appl. Polym. Sci.* **1970**, *14*, 2145.
(47) Fukutomi, T.; Tsukada, M.; Takurai, A.; Noguchi, T. *Polym. J.* **1972**, *3*, 717.
(48) Nakano, A.; Minoura, Y. *J. Appl. Polym. Sci.* **1975**, *19*, 2119.
(49) Goodman, J. *J. Polym. Sci.* **1957**, *25*, 325.
(50) Zakin, J. L.; Hunston, D. L. *Proceedings of the BHRA Conference on Drag Reduction, Cambridge* **1977**, *C5*, 41.
(51) Yu, J. F. S.; Zakin, J. L.; Patterson, G. K. *J. Appl. Polym. Sci.* **1979**, *23*, 2493.
(52) Frank, F. C. *Proc. R. Soc. London* **1970**, *A319*, 127.
(53) Cerf, R. *J. Chem. Phys.* **1951**, *48*, 59.
(54) Lumley, J. L. *Symp. Math.* **1972**, *9*, 315.
(55) Nguyen, T. Q.; Kausch, H. H. *Chimia* **1986**, *40*, 129.
(56) Bueche, F. *J. Appl. Polym. Sci.* **1960**, *4*, 101.
(57) Muller, A.; Odell, J. A.; Tatham, J., accepted for publication in *J. Non-Newtonian Fluid Mech.*
(58) Bywater, S.; Worsfield, D. J. *J. Polym. Sci.* **1962**, *58*, 571.

Registry No. aPS, 9003-53-6.